EUROPEAN FUSION DEVELOPMENT AGREEMENT

EFDA–JET–CP(04)07-06

R.J. Buttery, P. Belo, D.P. Brennan, S. Coda, L.-G. Eriksson, B. Gonçalves, J.P. Graves, S. Günter, C. Hegna, T.C. Hender, D.F. Howell, H.R. Koslowski, R. J. La Haye, M. Maraschek, M.L. Mayoral, A. Mück, M.F.F. Nave, O. Sauter, E. Westerhof, C.G. Windsor, the ASDEX Upgrade and DIII-D teams, and JET EFDA Contributors

Cross-Machine NTM Physics Studies and Implications for ITER

Cross-Machine NTM Physics Studies and Implications for ITER

R.J. Buttery[1], P. Belo[2], D.P. Brennan[3], S. Coda[4], L.-G. Eriksson[5], B. Gonçalves[2], J.P. Graves[4], S. Günter[6], C. Hegna[7], T.C. Hender[1], D.F. Howell[1], H.R. Koslowski[8], R.J. La Haye[3], M. Maraschek[6], M.L. Mayoral[1], A. Mück[4], M.F.F. Nave[2], O. Sauter[4], E. Westerhof[9], C.G. Windsor[1], the ASDEX Upgrade[6] and DIII-D teams[3], and JET EFDA Contributors*

[1]EURATOM/UKAEA Fusion Association, Culham Science Centre, Abingdon Oxon OX14 3DB, UK
[2]Association EURATOM/IST, Centre de Fusão Nuclear, 1049-001, Portugal
[3]General Atomics, P.O. Box 85608, San Diego, California, USA
[4]CRPP, Association EURATOM-Confédération Suisse, EPFL, 1015 Lausanne, Switzerland
[5]Association EURATOM-CEA, CEA-Cadarache, F-13108 St. Paul lez Durance, France
[6]MPI für Plasmaphysik, EURATOM Association, D-85748, Garching, Germany
[7]Department of Engineering Physics, University of Wisconsin, USA
[8]Association EURATOM-FZ Jülich IPP, Trilateral Euregio Cluster, 52425 Jülich, Germany
[9]FOM-Rijnhuizen, Ass. EURATOM-FOM, TEC, Nieuwegein, The Netherlands
** See annex of J. Pamela et al, "Overview of JET Results ", (Proc.20 [th] IAEA Fusion Energy Conference, Vilamoura, Portugal (2004).*

Preprint of Paper to be submitted for publication in Proceedings of the
20th IAEA Conference,
(Vilamoura, Portugal 1-6 November 2004)

“This document is intended for publication in the open literature. It is made available on the understanding that it may not be further circulated and extracts or references may not be published prior to publication of the original when applicable, or without the consent of the Publications Officer, EFDA, Culham Science Centre, Abingdon, Oxon, OX14 3DB, UK.”

“Enquiries about Copyright and reproduction should be addressed to the Publications Officer, EFDA, Culham Science Centre, Abingdon, Oxon, OX14 3DB, UK.”

ABSTRACT.
Control or avoidance of Neoclassical Tearing Modes (NTMs) will be necessary for good performance in ITER. Recent joint ITPA/IEA and other experiments on JET, DIII-D and ASDEX Upgrade are reported providing new insights into the transport effects, seeding, underlying physics, and threshold scaling of NTMs. Studies highlight the key role of sawteeth in triggering NTMs, with advances made in prediction and control in ITER-relevant high fast particle content plasmas. A range of trigger mechanisms are found in ELMy H-mode and hybrid scenarios, with 3 types of NTM impacting performance. Underlying physics scales towards increased NTM sensitivity in ITER, suggesting further measurement and development of control strategies are important.

1. INTRODUCTION - ISSUES AND IMPACT OF NTMS

The triggering of a Neoclassical Tearing Mode (NTM) is a complex process. Not only does it involve several subtle mechanisms governing the evolution of a neoclassical island. There also remain critical uncertainties both in the form, threshold and controllability of the triggering instability, and in the coupling process by which the triggering instability induces an initial island. Nevertheless, in recent years there has been considerable progress both in understanding the mechanisms and developing control over them.

For ITER, NTM triggering remains a crucial issue,as the mode is expected to account for the main β limit in H-mode and hybrid scenarios. The most serious concern is for sawtoothing ELMy H-modes, where the strong fast particle populations (from negative ion beams and fusion born a particles) are expected to partially stabilise sawteeth [1] leading to long periods. As seen on JET (Fig.1), such events can excite multiple types of NTM, at low β_N [2], leading to large falls in particle and energy confinement. Thus, issues that must be addressed for ITER include predicting and controlling mode thresholds, understanding their consequences, and the requirements for control or removal. We summarise progress on these fronts in this paper. Direct NTM stabilisation is discussed in other papers at this conference [3,4].

2. FORMALISM - NTM PHYSICS SCALINGS

To understand how the various physical mechanisms combine to trigger an NTM, it is useful to consider the modified Rutherford equation, which governs the evolution of an island of full width, w and minor radius, r [5,6]:

$$\frac{\tau_r}{r}\frac{dw}{dt} = r(\Delta' - \alpha w) + r\beta_P\left[a_{bs}\left(\frac{0.65\,w}{w^2 + w_d^2} + \frac{0.35\,w}{w^2 + 28\,w_b^2}\right) - \frac{a_{GGJ}}{\sqrt{w^2 + 0.2\,w_d^2}} - \frac{a_{pol}\;w}{w^4 + w_b^4}\right] \qquad (1)$$

Here the NTM is driven by a helical hole in the bootstrap current [7] around an island (the a_{bs} term) and so is dependent on the local poloidal β, β_p (with a small correction for field curvature [8], a_{GGJ} term). Islands rapidly grow (on a resistive timescale, τ_r) to a saturated size which to first order depends on the ratio of the bootstrap term to the classical tearing stability index [the $r(\Delta'-\alpha w)$

term], which by definition is negative for an NTM (the coefficient a describing its island size dependence [9]). However, the w_d, a_{pol}, and terms make the NTM unconditionally stable at small island size (and also low β) leading to the requirement of a seeding event to induce a large enough island for neoclassical growth. These small island terms are due respectively to (w_d) the effects of finite transport over the island [10], (a_{pol}) ion polarisation currents [11], and (w_b) the loss of bootstrap as size approaches ion banana widths [12]. They are important both in governing the thresholds for the modes, and the requirements for NTM control systems. Most significantly they lead to a dependence on normalised poloidal Larmor radius, ρ*, which is expected to play a key role in the scaling of NTM physics towards ITER. For example, the ion polarisation current term can be characterised by [13],

$$a_{pol} \propto g(\nu,\varepsilon)\,(L_q/L_p)^2\,\rho_{i\theta}^2\,.\;\Omega(\Omega-\omega_i^*)/\omega_e^{*2} \qquad (2)$$

where 'g' is a function of normalised collisionality, $\nu = \nu_i/\varepsilon\omega_e^*$, with g=1 for n<<1, and $g=\varepsilon^{-3/2}$ for ν >>1; ni is the ion collision frequency, ω_e^* (ω_i^*) is the electron (ion) diamagnetic frequency, and $\rho_{i\theta}$ is the poloidal Larmor radius, all taken at the resonant surface. This depends on the natural island propagation frequency (Ω) in the zero radial electric field frame of reference [13] which is somewhat uncertain both experimentally and theoretically. Nevertheless, folding this back into Eq. (1), assuming a given seed size, $w = w_{seed}$, solving for marginal growth (dw/dt = 0), and neglecting rotation, w_d and w_b terms, gives a threshold for NTM onset in β_p which scales with ρ*:

$$\sqrt{\frac{L_q}{L_q}}\;\beta_{p-onset} = -\,r_s\Delta'\,.\,\rho_{i\theta}^*\,.\,\frac{w_{seed}/w_{pol}}{[1-(w_{pol}/w_{seed})^2]}\;.\,g(\nu,\varepsilon) \qquad (3)$$

where $w_{pol}^2 = a_{pol}/(a_{bs}\varepsilon^{1/2}\,L_q/L_p)$ and $\rho_{i\theta}^* = \rho_{i\theta}/r_s$. A similar form can be obtained with the finite island transport model (w_d), as discussed in Refs [14] and[15], assuming a heat flux limited approach to allow for low collisionality [10].

3. ROLE OF THE SAWTOOTH IN NTM ONSET

The above argument assumes that variations in the physics terms in equation (1) dominate in NTM onset. However considerable uncertainty exists in the mechanisms that lead to a seed, and it can be speculated that as plasma heating is increased the processes which generate this seed might change considerably. This has recently been explored in Ref. [16], examining data from the JET tokamak. Here it is found (Fig.2) that simple ρ*– ν based scalings are in fact entirely non-predictive of the β at which the 3/2 NTM (denoted as poloidal/toroidal mode number) is triggered. Instead NTM onsets align with the normal discharge evolution (Fig.3) as β rises and the natural beam fuelled density evolves - additional parameters must control the point of NTM onset. Neural network techniques were employed to explore a wide range of possible control parameters; an automatic optimisation

found best network performance with just 3 parameters: β_N, $\rho_{i\phi}$*, and sawtooth period, as shown in Fig 4. Unlike ρ*– ν scalings used in Fig 2, this network clearly anticipates the approaching NTM, even though the discharges divide into two categories (upper group with onset during a rapid β rise; lower group with onset at higher β where discharges evolve more slowly). Exploring network performance (Table I) it is found that the number of errors (trajectories entering the yellow region in Fig.4) rises significantly if sawtooth period is removed, while ρ* offers little benefit. (Note that while collisionality does not enter into scalings on JET, it is found to play some role on other devices).

Given a choice between sawtooth period and magnetic precursor size, the network finds period most significant. This is also observed phenomenologically [2], with long sawteeth not having larger precursors. The β dependence is shown in Fig.5, which indicates an apparent threshold in sawtooth period above which NTM onset can occur close to the β threshold for metastability.

4. PREDICTION AND CONTROL OF SAWTEETH

In a burning plasma, it is expected that the strong energetic a population will stabilise sawteeth, leading to large infrequent events that trigger the NTM at low β_N - an effect observed directly on JET with ICRH accelerated ^{4}He ions [17]. The importance of sawtooth control is highlighted by recent experiments on JET. Here it is found that low β NTMs (eg blue curves in Fig.1) could be avoided by utilising two strategies: firstly, ICRH phasing was switched to one that reduced the core particle pinch (-90^o). Secondly the timing of the heating power rise was delayed to establish a sawtoothing auxiliary heated L-mode, prior to H-mode entry. This is conjectured to reduce profile peaking in the core before introduction of strong fast particle populations, and thereby avoid a long first sawtooth that triggers the NTM. This led to dramatically reduced mode activity with improved performance and stable operation at much higher input power, as shown in the red case in Fig.1. Thus careful consideration of plasma profiles and operational development can!Cvoid the most severe effects of NTMs.

For ITER sawteeth, two strategies are possible: (i) stabilisation with early a production, or (ii) destabilisation to make them small and benign. Latest estimates [18] suggest the former can delay the first sawtooth for perhaps 50s, allowing thermal equilibration. Significant extensions may be possible with aggressive current drive techniques [19] or modifications to the start-up, but these change the scenario, and leave the ability to reach steady state or test materials, limited. Sawtooth destabilisation was demonstrated on JET using Ion Cyclotron Current Drive (ICCD) to modify $q = 1$ shear in the 1990s [20], and raise NTM thresholds in 2000 [2]. However, these results were obtained in regimes without significant fast particles, where the sawtooth crash occurs when the most unstable *resistive* internal kink exceeds diamagnetic frequencies, yielding a criterion in terms of local shear [21]. For fast particle stabilised sawteeth the crash depends on the size of stabilising contributions to the potential energy (ie *ideal* MHD). It was unclear theoretically whether this different process could be influenced significantly by local shear modifications.

This question has now been answered by new experiments on JET using two ‘flavours’ of ICCD [22] (Fig.6): one (in red) to generate strong core fast particle populations and large sawteeth, the

other (in green) to drive localised current at the q = 1 surface. It is found that as the current drive location (green) approaches the sawtooth inversion radius (blue dotted), the sawtooth period (light blue) and amplitude (dark blue) fall dramatically. Conversely, for cases with other ICCD phasings or deposition locations the sawteeth are not destabilised, demonstrating the effect to be due to localised current drive. These results put sawtooth destabilisation in ITER on a much firmer footing. They are complemented by progress on ASDEX Upgrade using electron cyclotron current drive (the likely tool for this in ITER), discussed at this conference in Ref [3]. Work is now required to integrate these control techniques into high fast particle baseline demonstrations at high β.

For ITER, there are additional concerns, and opportunities, arising from the highly energetic (~1MeV) negative ion neutral beams (NNB). Although these might be expected to have a weak effect on sawteeth, due to their tangential injection giving less trapped ions, experiments on JT-60U [23] with 350keV NNB demonstrated significant sawtooth stabilisation. These results were explained by Graves [24], finding new finite orbit effects from ions intersecting the $q = 1$ surface - these change the free energy available to drive the instability. Thus with core co-injection the internal kink has a high critical bp to be triggered (Fig.7), leading to a long build up and large sawtooth crash. However, the results also show that off-axis co-injection (dashed line) can reverse the fast ion pressure gradient at $q = 1$ and lower the β_p threshold. This provides a new mechanism for sawtooth destabilisation in ITER, although it should be noted that off-axis injection can also change current profiles and shear near q=1, potentially modifying this effect [19].

A further influence arises with strong neutral beam momentum injection, due to stabilising kinetic effects at high plasma rotation. Although not likely to be a factor in ITER, it is vital to take account of this in modelling present devices, as it can lead to substantially longer sawtooth periods. This has recently been measured on JET (Fig.8(a)) where results show qualitative consistency with earlier predictions [25] of the critical β_p for triggering a sawtooth (Fig.8(b)). Taken together, the above results show that a quantitatively predictive theory for sawteeth is developing well, and that the required 'monster' sawtooth destabilisation is achievable, and could be developed as a tool prior to ITER operation.

5. THE SEEDING PROCESS

Central to understanding and predicting NTM onset is the seeding process by which an MHD event or boundary triggers an NTM. Here we find a range of possible mechanisms, as might be expected from the observation of a low metastability threshold for NTMs in present devices. It is important to explore and resolve these for ITER.

Early seeding models focussed on the possibility of magnetic coupling, for example between the sawtooth precursor and NTM resonant surface, exciting an island that would then grow neoclassically [26]. Indeed, 3/2 NTMs are often triggered during extended phases of sawtooth precursor activity, usually near its peak amplitude [27]. The mode frequencies generally preclude toroidal coupling to n = 2 sawtooth precursors, but a further possibility [28] lies in 'three wave' coupling between 1/1 sawtooth

precursors, 4/3 NTMs, and the q = 3/2 surface. Here rotation frequencies are generally better matched, and indeed such coupling is highlighted in some cases by bicoherence analyses of JET data showing clear phase locking between driving (4/3 and 1/1) and driven (3/2) perturbations (Fig.9). However, such frequency matches are not always established, or correlated with NTM growth. Thus, Hegna has proposed a mechanism based on the transient changes to the transport properties around a magnetic island resulting from MHD events [29]. The model relies on the existence of neoclassical polarisation currents whose stability properties depend on the island rotation frequency in the **E**×**B** rest frame. The theory accounts for the competing dissipative mechanisms that influence the island rotation. An MHD event can transiently increase the electron dissipation and cause the island to rotate in the electron diamagnetic direction. This affects the sign and amplitude of the neoclassical polarisation currents that influence nonlinear evolution as described by a_{pol} in Eq. (1). Hence, MHD events may transiently eliminate the polarisation threshold mechanism and lead to island growth. This theory may explain cases on JET where NTM growth correlates with sawtooth precursor activity without frequency matching [27], and also DIII-D results of error fields lowering 2/1 NTM thresholds.

With longer sawteeth, NTMs appear at lower β_N, often directly at the sawtooth crash (Fig.1). Such events are likely to be a result of forced reconnection. This has been explored in modelling by Brennan (Fig.10) using typical DIII-D parameters and profiles. Here, the relative rotation between q = 1 and q = 1.5 surfaces is important with the model showing that although this reduces the size of the 3/2 mode, it is still driven unstable. Initial mode structure conforms to linear predictions, but becomes contorted by the flow in the non-linear phase (box in Fig.10), beginning to flatten temperature profiles. This work shows promising indications of a viable mechanism for NTM seeding by forced reconnection, being one of the first studies of growth from near zero island size. Studies must now be extended to higher $S \sim 10^8$ (greater computational power) and include further physics terms.

The most serious impact on performance comes from 2/1 NTMs. These generally occur above 3/2 NTM thresholds, although with large sawteeth the chances of obtaining a 2/1 NTM are greatly increased. At high β_N, 2/1 NTMs can be triggered by sawteeth or ELMs (especially at lower q_{95}), but do not always require a triggering instability [30]. Although β thresholds align to a ρ^* scaling, modes most commonly occur close to the with-wall β limit. This has driven the adoption of a theory based on poles in the classical tearing stability, Δ', which develop as ideal limits are approached. Its application to NTMs was demonstrated for DIII-D [31], where it was found that Δ' slowly evolves towards instability as β_N rises towards the ideal β limit. This has also been extended to explain high β_N sawtooth triggered 3/2 NTMs [32], where the sawteeth help drive the island growth as the plasma approaches a Δ' pole from the $n = 2$ ideal pressure driven kink.

A further influence on 2/1 NTM thresholds originates from error fields (which arise from design asymmetries in a tokamak). On JET, error fields lowered 2/1 NTM β_N thresholds by ~35% and caused them to start in a locked state. This indicates that the two drives for island growth combine, with increased error field sensitivity (and plasma braking) at high β_N. A similar effect is seen on DIII-D (Fig.11), although in this case there is a substantial region of lower NTM β thresholds with

the mode still formed rotating. This suggests a more subtle mechanism, with the error field altering the NTM drive, rather than directly driving the island itself (which requires the island to be locked to the error field). Indeed preliminary rotation data indicates decreased plasma rotation in the **E**×**B** rest frame, potentially reducing ion polarisation current effects and enabling seeding.

Fishbones also trigger NTMs. While early results from ASDEX Upgrade [33] showed 3/2 NTM onset β vs ρ^* scalings to be ~20% with fishbones instead of sawteeth, new JET data (Fig.12) shows with more fast particles and shaping, fishbone triggered NTMs do not extend to lower β_N (as sawteeth do). Also, JET fishbone cases appear (unlike in ASDEX Upgrade) to follow the same trajectory as sawtooth seeded cases - this trajectory arises from the natural evolution, confinement and beam fuelling of the discharges. In addition fishbones have been recently observed to trigger 2/1 NTMs at high β_N (~2.5) in JET hybrid scenarios.

6. SCALING OF THE UNDERLYING NTM PHYSICS

With a range of seeding mechanisms, the underlying criteria for neoclassical growth becomes crucial, with the key question being how do the small island terms scale towards ITER? These not only govern the sensitivity to triggering events, but also the requirements for control of small islands and their removal by electron cyclotron systems in ITER. By performing β ramp-down experiments, and fitting consequent island size evolutions using Eqn (1), it is possible to empirically measure the size and scaling of these small island effects, allowing direct extrapolation to ITER. New 'ITPA' cross-machine experiments have been executed on JET, DIII-D and ASDEX Upgrade, to address this for the 3/2 NTM. Results show a clear trend with the metastability β threshold (Fig.14, plotted in local parameters related to the underlying NTM bootstrap drive) falling with normalised poloidal ρ^*. Preliminary analysis also suggests that scale lengths for small island stabilisation terms do not vary substantially with $\rho_{i\theta}^*$ (Fig.15). This suggests a challenging task for ITER, operating well above the metastability threshold, with complete NTM removal requiring ECCD to drive island sizes down to levels similar to those required in present devices. Similar work is continuing for the 2/1 NTM.

7. CONSEQUENCES OF NTMS AND IMPLICATIONS FOR ITER

With various trigger mechanisms and NTM types, it is important to understand NTM consequences. 2/1 NTMs clearly have the most serious impact (Fig.1) and are unacceptable to ITER [34]. However, 3/2 NTMs are also significant and could impact fusion power substantially [34] (although they are ubiquitous and fairly benign in hybrid scenarios). Effects have been explored further in JET trace Tritium experiments, using horizontal and vertical neutron cameras to track the progress of a Tritium puff, constraining transport simulations. Preliminary results show the 3/2 NTM consistent with a ~50% reduction in the inward pinch in the vicinity of the island [35]. However, recent work has also shown that at low q_{95}, even higher harmonic NTMs can have a significant effect. For example in JET Pulse No: 62129 (Fig.16, 3.7MA, 2.9T, q_{95} = 2.7) successively higher number modes are associated with steps in confinement and neutron rate. With the 4/3 NTM present, neutron rates are

~30% lower than values once all the modes have disappeared, while stored energy is ~13% lower. Although there is a slight evolution in current profile (linked with and probably driving, the appearance and decay of each mode), the ELMs and plasma density remain fairly constant. Thus it seems likely that the high *m*/*n* modes are accounting for most of this behaviour.

Thus we see a range of NTMs and triggering mechanisms pose a concern for ITER. But we also see that the problem is becoming tractable, with benign scalings for some events (eg a β_N limit), and the possibility of control when scalings are adverse. In baseline scenarios the most serious limit originates from sawteeth, where there is good progress in predicting and controlling behaviour. Further triggers (fishbones, Δ' poles, and possibly ELMs) occur at higher β_N, but it seems at least possible that these will be at similar bN in ITER. In the hybrid scenario, the main concern remains the 2/1 NTM at high β_N - the extrapolation of this needs to be tested for ITER. Pre-emptive current drive at the NTM resonant surface can also raise NTM onset bs, as recently shown in DIII-D with real time MSE tracking of q = 3/2 [36]. However, with theory predicting greatly increased sensitivity to NTMs in ITER, due to its low ρ^*, we must not be complacent. There remain many aspects that need further theoretical and experimental elucidation, not least, the seeding. Further, strong α and NNB fast particle populations, will make sawtooth control challenging. So, while the principal physics ingredients *may* have been assembled, and a new generation of codes is developing, work now needs to focus on measuring and explaining events in detail in order to predict behaviour and requirements for ITER. Control techniques must also be developed as robust, ready to use tools, rather than lengthy research programmes for ITER. Thus, NTM physics remains as a challenging and serious issue for ITER, but one in which progress is beginning to pay off in terms of theoretical and experimental tools to predict and control behaviour.

ACKNOWLEDGEMENTS

This work was jointly funded by EURATOM, the UK EPSRC, the US DoE under contract DE-FC02-04ER54698, the Swiss National Science Foundation, and partly performed under the European Fusion Development Agreement. Thanks to A. Kavin and A. Polevoi for ITER data.

REFERENCES

[1]. Campbell, D.J., et al. Phys.Rev.Lett. **60**(1988)2148.
[2]. Sauter, O. et al. Phys.Rev.Lett. **88** (2002) 105001.
[3]. Maraschek, M., et al. this conference.
[4]. Petty, C., and Humphrey S, D., this conference.
[5]. Carrera, R., et al. Phys. Fluids **29** (1986) 899.
[6]. Sauter, O., et al. Phys. Plas. **4**, (1997) 1654.
[7]. Sauter, O.,et al.Phys.Plas.**6**(1999)2834;**9**(2002)5140.
[8]. Lutjens, H., et al. Phys. Plasmas **8**, (2001) 4267.
[9]. White, R.B., et al. Phys. Fluids **20**, (1977) 800.

[10]. Fitzpatrick, R., et al. Phys. Plas. **2**, (1995) 825.
[11]. Wilson, H.R., et al. Phys. Plasmas **3**, (1996) 248.
[12]. Poli, E., et al. Phys. Rev. Lett. **88** (2002) 075001.
[13]. Wilson, H.R.,et al.Plas.Phys.Con.Fus.**38**(1996)A149.
[14]. La Haye, R.J., et al. Phys. Plas. **7** (2000) 3349.
[15]. Zohm, H. et al. Phys. Plas. **8** (2001) 2009.
[16]. Buttery, R.J., et al. Nuc. Fus., **44** (2004) 678.
[17]. Paméla, J., et al. Nuc. Fus. **42** (2002) 1014.
[18]. Porcelli, F., et al. Nuc. Fus. **44** (2004) 362.
[19]. Muuck, A., et al. Proc.30th EPS, ECA **27A**, P-1.131.
[20]. Bhatnagar, V.P., et al. Nuc.Fus.**34**(1994)1579.
[21]. Porcelli,F.,et al. Plas.Phys.Con.Fus.**38**(1996)2163.
[22]. Eriksson, L.G.,et al.Phys.Rev.Lett.**92**(2004)235004.
[23]. Kramer, G.J., et al. Nuc. Fus. **40** (2000) 1383.
[24]. Gravse, J.P., Phys. Rev. Lett. **92** (2004) 185003.
[25]. Graves, J.P., et al. Plas.Phys.Con.Fus.**42**(2000)1049.
[26]. Hegna, C.C., et al. Phys. Plas. 6 (1999) 130.
[27]. Buttery, R.J. et al. Nuc. Fus. **43** (2003) 69.
[28]. Nave, M.F.F., et al, Nuc. Fus. **43** (2003) 179.
[29]. Hegna, C.C., Bull. Am. Phys. Soc. **48** (2003) 280.
[30]. Hnder, T.C., et al. Nuc. Fus. **44** (2004) 788.
[31]. Brennan, D.P., et al. Phys. Plas. **9** (2002) 2998.
[32]. Brennan, D.P., et al. Phys Plas **10** (2003) 1643.
[33]. Gude, A., et al. Nuc. Fus. **39** (1999) 127.
[34]. Buttery, R.J., et al.Plas.Phys.Con.Fus.**42**(2000)B61.
[35]. Hender, T.C., et al.Proc.31st EPS **28G** ECA P-1.163.
[36]. La Hayer, R.J., et al.Proc.31st EPS **28G** ECA P-2.181.

Parameters used:	**Residual**[1]	**Errors**
$\beta_N\ \tau_{sawtooth}\ \rho_{i\phi}$*	34.3	17%
$\beta_N\ \tau_{sawtooth}$	34.4	20%
$\beta_N\ \rho_{i\phi}$*	35.7	26%
β_N	35.9	31%
$\rho_{i\phi}$*	37.5	29%

[1]Σ (predicted - actual time to NTM)^2

TABLE I: Neural network error dependence on input parameters.

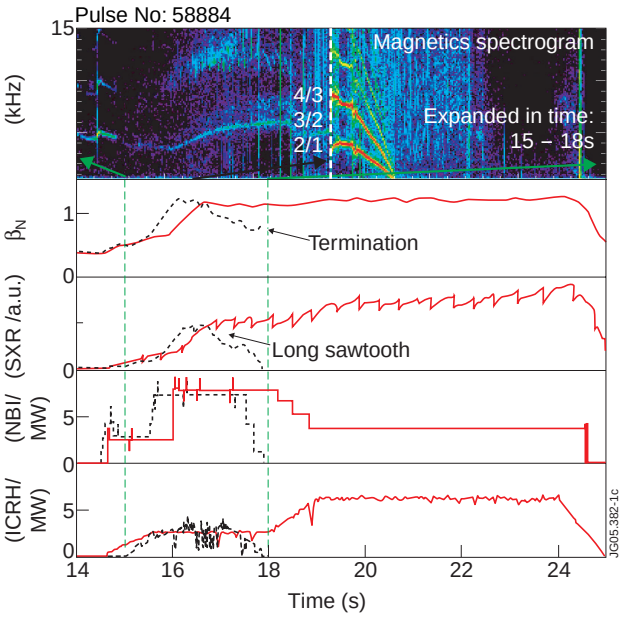

Figure 1: Multiple NTMs excited by long sawtooth crash at low β_N (Pulse No: 58884 in blue), and a no-NTM case (Pulse No: 58893 in red) in JET.

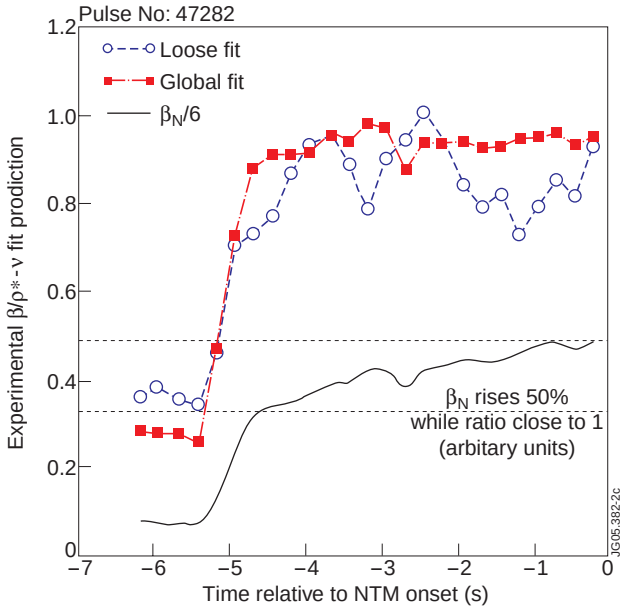

Figure 2: Ratio of β in Pulse No: 47282 to value predicted for NTM onset from power law β(ρ, ν) fits to JET data.*

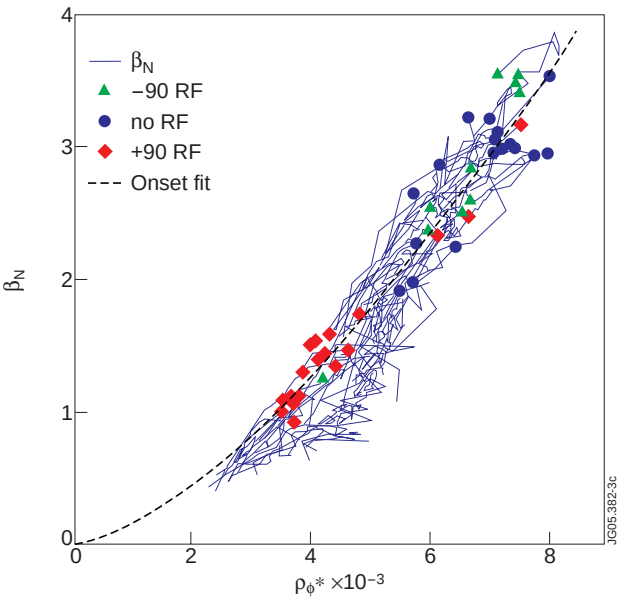

Figure 3: NTM onsets (symbols) and discharge trajectories (lines) for shots with/without ICRH heating as in key.

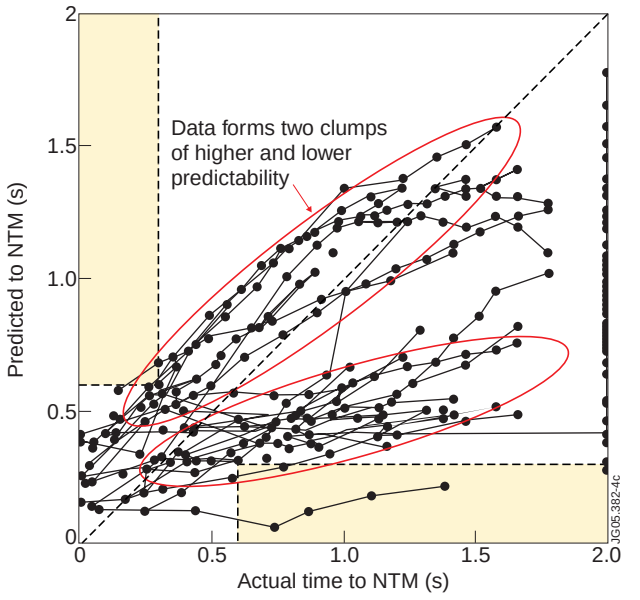

Figure 4: Comparison of optimal neural network NTM onset prediction with actual time to NTM.

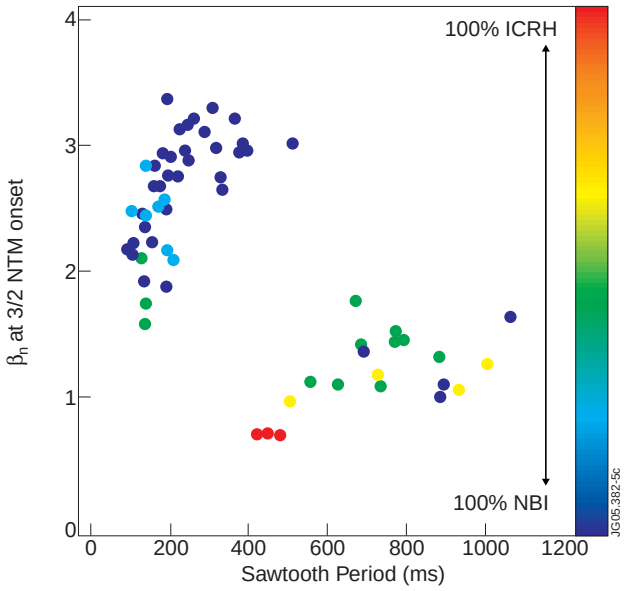

Figure 5: Dependence of 3/2 NTM onset β_N on $\tau_{sawtooth}$ and heating mix (colour) in JET.

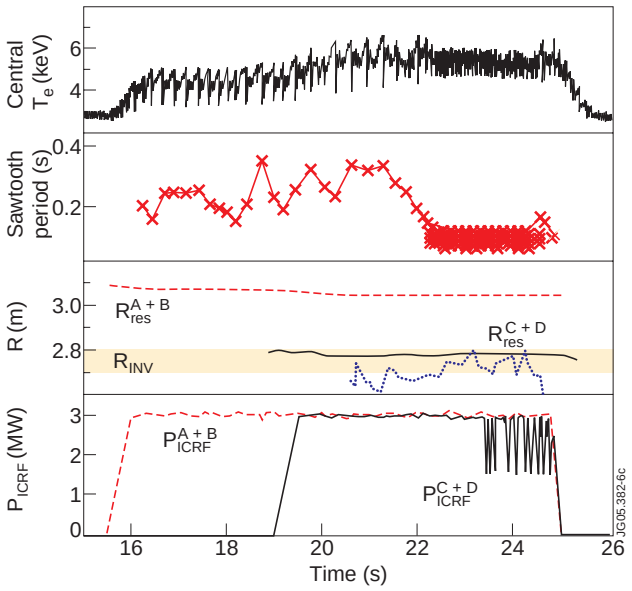

Figure 6: Effect of q=1 current drive on ICRH stabilised sawteeth (see text).

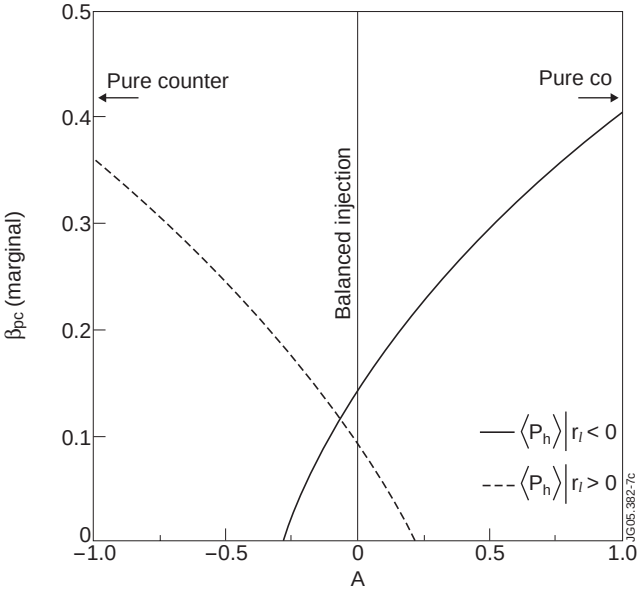

Figure 7: Critical β_p for sawtooth crash as a function of beam injection asymmetry (A) for injection on axis (solid) and just outside q=1 (dashed).

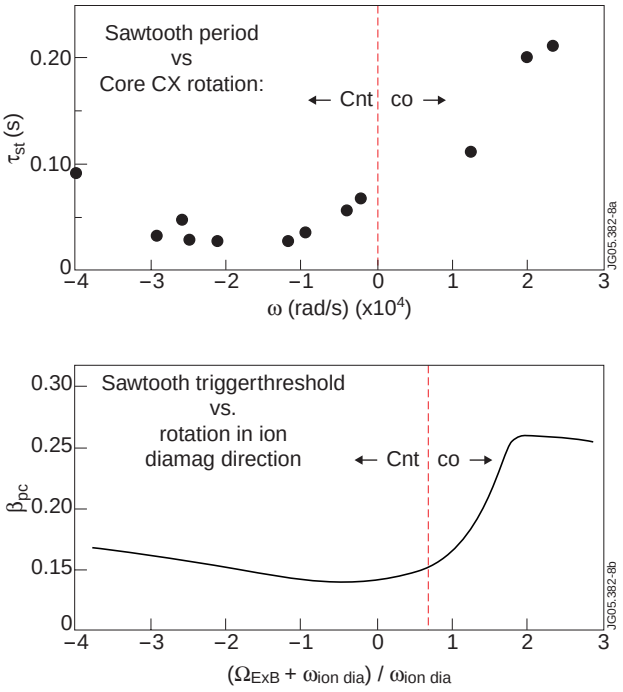

Figure 8: a) Sawtooth period versus plasma rotation for neutral beam co/counter injection at various power levels on JET; b) Critical β_p for ideal internal kink as a function of normalised plasma rotation.

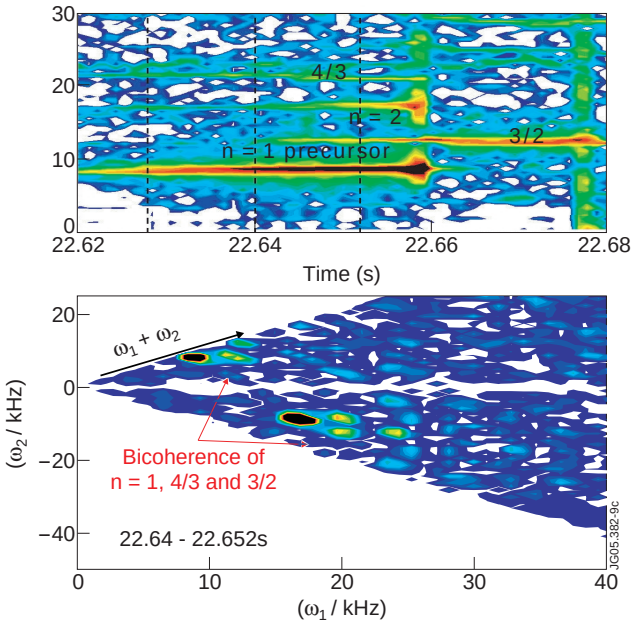

Figure 9: Spectrogram and bicoherence plots for JET Pulse No: 51995.

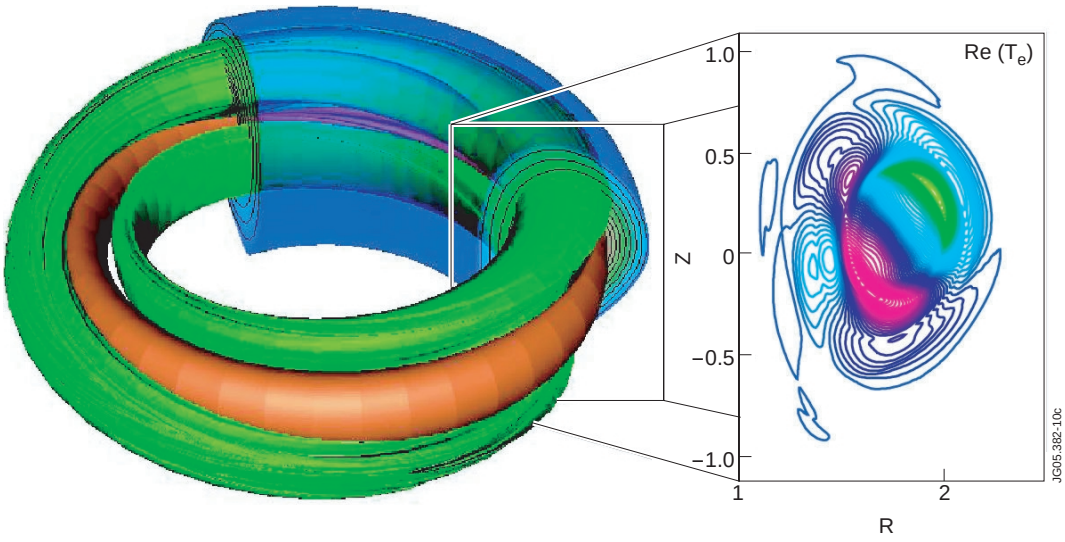

Figure 10: Isosurface of perturbed n = 1 pressure (orange) and n = 2 toroidal current (green), and perturbed electron temperature (box) in the nonlinear phase of a simulated sawtoothing DIII-D discharge

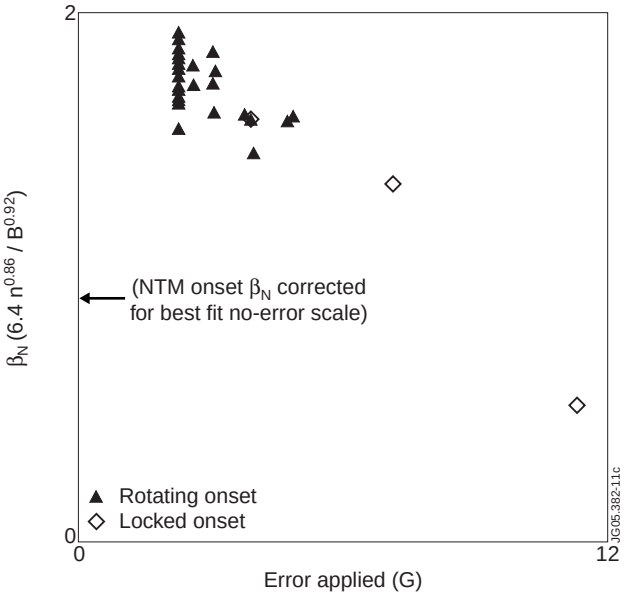

Figure 11: Effect of applied error field on 2/1 NTM threshold on DIII-D.

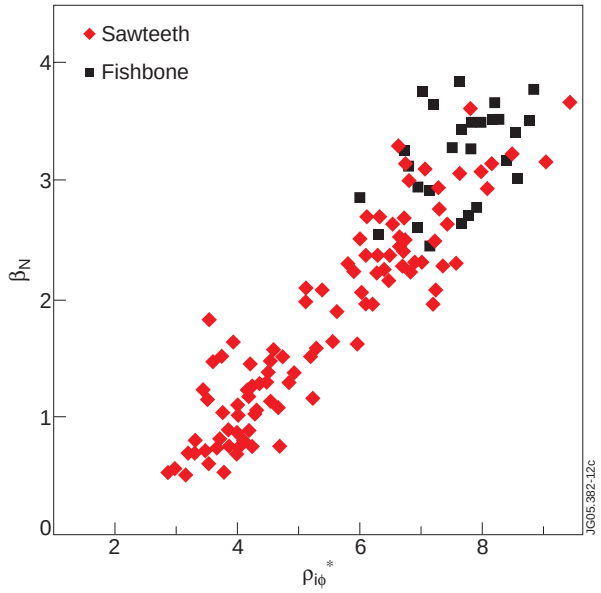

Figure 12: Fishbone and sawtooth seeded 3/2 NTMs onset bN in JET

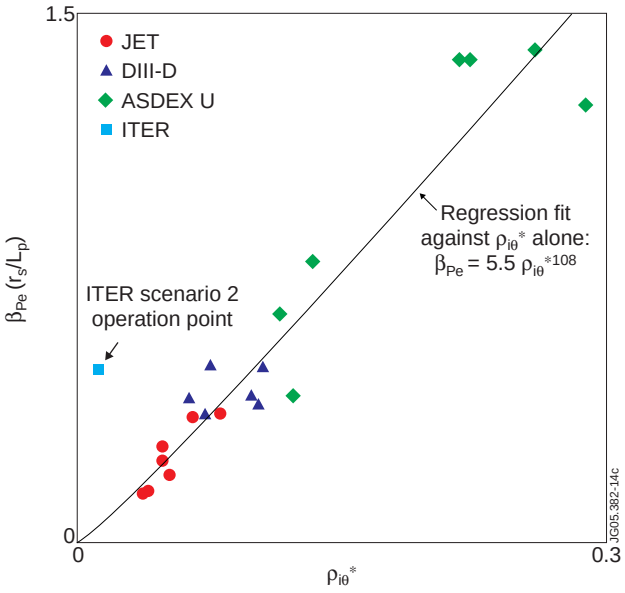

Figure 14: 3/2 NTM metastability threshold scaling plotted against normalised poloidal ion Larmor radius.

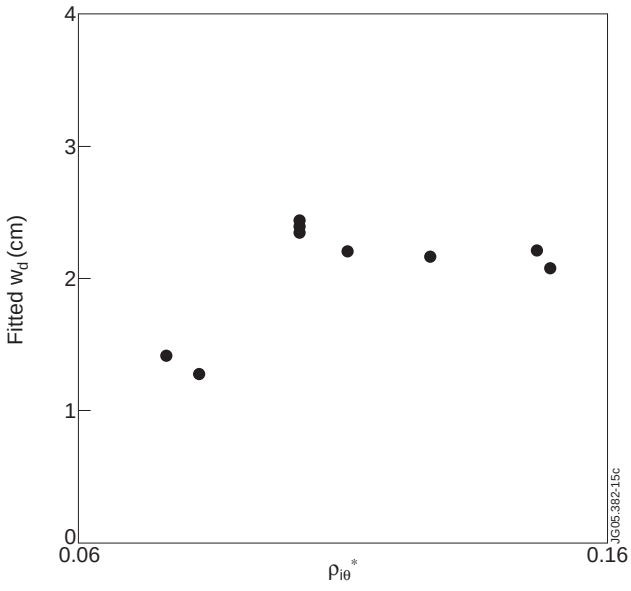

Figure 15: $\rho_{i\theta}$ dependence of wd (DIII-D).*

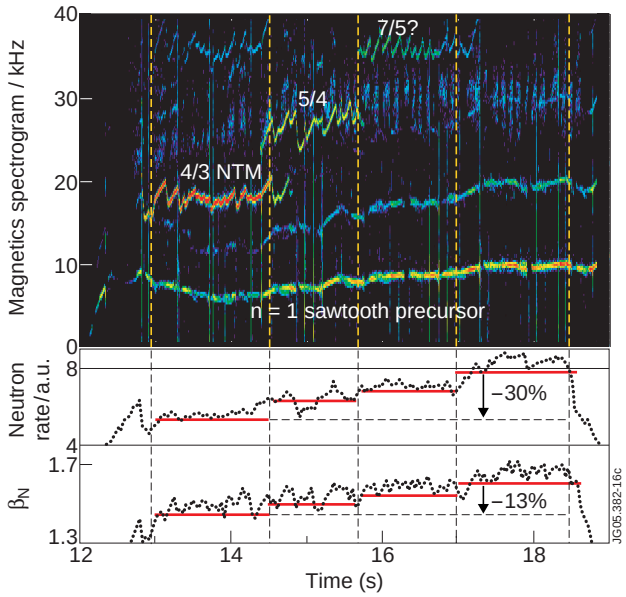

Figure 16: Evolution of discharge with modes at constant heating power in JET Pulse No: 62129.